

Digital Reaction-Diffusion System—A Foundation of Bio-Inspired Texture Image Processing—

Koichi ITO^{†a)}, *Student Member*, Takafumi AOKI[†], *Regular Member*,
and Tatsuo HIGUCHI[†], *Fellow*

SUMMARY This paper presents a digital reaction-diffusion system (DRDS)—a model of a discrete-time discrete-space reaction-diffusion dynamical system—for designing new image processing algorithms inspired by biological pattern formation phenomena. The original idea is based on the Turing's model of pattern formation which is widely known in mathematical biology. We first show that the Turing's morphogenesis can be understood by analyzing the pattern forming property of the DRDS within the framework of multidimensional digital signal processing theory. This paper also describes the design of an adaptive DRDS for image processing tasks, such as enhancement and restoration of fingerprint images.

key words: *reaction-diffusion system, pattern formation, digital signal processing, digital filters*

1. Introduction

Living organisms can create a remarkable variety of structures to realize their intelligent functions. At present, we have only limited understanding of the mechanism of *morphogenesis*—the development of patterns and forms in living systems. Recently, model-based studies of morphogenesis employing computer simulations have begun to attract much attention in mathematical biology [1], [2]. From an engineering point of view, the insights into morphogenesis provide important concepts for devising a new class of intelligent signal processing algorithms employing biological pattern formation capability. Motivated by this viewpoint, several examples of signal processing algorithms inspired by biological pattern formation mechanism have been proposed [3]–[5].

Many biological pattern formation phenomena can be described and modeled mathematically by reaction-diffusion equations. In 1952, Alan Turing suggested an important idea of *diffusion-driven instability* or *Turing instability* for understanding the principle of morphogenesis. Following the Turing's model, most of computational models of biological pattern formation (for both scientific and engineering applications) are described by continuous-time reaction-diffusion equations, and hence can not be directly handled by the the-

ory of digital signal processing. Addressing this problem, this paper proposes a *Digital Reaction-Diffusion System* (DRDS)—a model of a discrete-time discrete-space reaction-diffusion dynamical system, which is useful for designing new types of signal processing algorithms based on biological pattern formation mechanism. The goal of this study is to construct a framework of *digital morphogenesis* for manipulating texture images, patterns, and structures appeared in signal processing and computer graphics applications.

The behavior of DRDS can be analyzed systematically within the framework of multidimensional digital signal processing. In Sect. 2 and Sect. 3, we first show that the Turing's scenario of pattern formation can be naturally understood by the stability analysis of multidimensional digital systems. Section 4 extends the original DRDS to an adaptive DRDS, and presents its application to enhancement and restoration of fingerprint images. Our emphasis is that the discretization of continuous reaction-diffusion system to obtain the model of DRDS, which is the main contribution of this work, allows a good combination of biological pattern formation models and general image filtering techniques. This approach may provide a useful foundation for designing new image/texture processing algorithms.

2. Reaction-Diffusion System

2.1 Turing's Model of Pattern Formation

It is suggested that a system of chemical substances, called *morphogens*, reacting together and diffusing through a tissue plays an important role in biological pattern formation. Spatial patterns in chemical reactions arise mainly from the interaction between reaction kinetics and diffusion of different substances. Instability in respect to diffusion plays an essential role here as first suggested by Alan Turing. Turing demonstrated that homogeneous chemical systems could become unstable with respect to concentration fluctuations of finite wavelength and evolve into spatially periodic patterns. We consider here reaction-diffusion systems for two chemical substances in the form:

Manuscript received December 9, 2000.

Manuscript revised March 5, 2001.

[†]The authors are with the Department of System Information Sciences, Graduate School of Information Sciences, Tohoku University, Sendai-shi, 980-8579 Japan.

a) E-mail: ito@higuchi.ecei.tohoku.ac.jp

$$\begin{cases} \frac{\partial X}{\partial t} = F(X, Y) + D_X \nabla^2 X \\ \frac{\partial Y}{\partial t} = G(X, Y) + D_Y \nabla^2 Y \end{cases}, \quad (1)$$

where X and Y are concentrations of two chemical substances, F and G account for nonlinear reaction kinetics, and D_X and D_Y are the diffusion coefficients of X and Y , respectively. Consider the condition under which the system (1) can exhibit instabilities around the equilibrium. Let assume that concentration vector (X, Y) can be written: $X = X_0 + x$ and $Y = Y_0 + y$, where (X_0, Y_0) is the equilibrium of the system. In the neighborhood of the equilibrium, the linearized equation for (1) is given by

$$\frac{\partial}{\partial t} \begin{bmatrix} x \\ y \end{bmatrix} = \begin{bmatrix} F_X + D_X \nabla^2 & F_Y \\ G_X & G_Y + D_Y \nabla^2 \end{bmatrix} \begin{bmatrix} x \\ y \end{bmatrix}, \quad (2)$$

where $F_X = \left(\frac{\partial F}{\partial X}\right)_{(X_0, Y_0)}$, etc. Let assume the solution of (2) can be written

$$\begin{cases} x = x_0 e^{\lambda t + j\mathbf{q} \cdot \mathbf{r}} \\ y = y_0 e^{\lambda t + j\mathbf{q} \cdot \mathbf{r}} \end{cases}, \quad (3)$$

where

- \mathbf{q} : the spatial wavevector,
with the wavenumber $|\mathbf{q}| = q$,
- \mathbf{r} : the position vector in continuous space.

With the solution (3), Eq. (2) can be rewritten as

$$\lambda \begin{bmatrix} x_0 \\ y_0 \end{bmatrix} = \begin{bmatrix} F_X - D_X q^2 & F_Y \\ G_X & G_Y - D_Y q^2 \end{bmatrix} \begin{bmatrix} x_0 \\ y_0 \end{bmatrix}. \quad (4)$$

The stability properties of the fixed point are determined by the eigenvalues λ of the 2×2 matrix in the above equation. Consider first the condition of reaction kinetics such that the fixed point (X_0, Y_0) is stable in the absence of diffusion (effectively $D_X = D_Y = 0$). This requires the real part of every eigenvalue (under $D_X = D_Y = 0$) must be negative, thus we have

$$F_X + G_Y < 0, \quad F_X G_Y - F_Y G_X > 0. \quad (5)$$

When we couple the reaction kinetics with spatial diffusion, the system can become unstable even if the original reaction kinetics (without diffusion) is stable. This type of instability is called *diffusion-driven instability*, where some eigenvalues become real and positive due to the effect of non-zero diffusion coefficients (D_X and D_Y). In the above example, this condition can be represented by

$$(F_X - D_X q^2)(G_Y - D_Y q^2) - F_Y G_X < 0, \quad (6)$$

for some $q \neq 0$. This instability initiates the growth of spatial structure characterized by the unstable mode of wavenumber q .

2.2 N -Morphogen Reaction-Diffusion Systems

This subsection describes a unified approach for analyzing the general N -species reaction-diffusion system with two-dimensional (2-D) space indices (r_1, r_2) , which is written as

$$\frac{\partial \tilde{\mathbf{x}}(t, r_1, r_2)}{\partial t} = \tilde{\mathbf{R}}(\tilde{\mathbf{x}}(t, r_1, r_2)) + \tilde{\mathbf{D}} \nabla^2 \tilde{\mathbf{x}}(t, r_1, r_2), \quad (7)$$

where

$$\tilde{\mathbf{x}} = [\tilde{x}_1, \tilde{x}_2, \dots, \tilde{x}_N]^T$$

\tilde{x}_i : concentration of the i -th morphogen

$$\tilde{\mathbf{R}}(\tilde{\mathbf{x}}) = [\tilde{R}_1(\tilde{\mathbf{x}}), \tilde{R}_2(\tilde{\mathbf{x}}), \dots, \tilde{R}_N(\tilde{\mathbf{x}})]^T$$

$\tilde{R}_i(\tilde{\mathbf{x}})$: reaction kinetics for the i -th morphogen

$$\tilde{\mathbf{D}} = \text{diag}[\tilde{D}_1, \tilde{D}_2, \dots, \tilde{D}_N]$$

diag: diagonal matrix

\tilde{D}_i : diffusion coefficient of the i -th morphogen.

In this paper, we focus on the 2-D reaction-diffusion system to discuss 2-D pattern formation.

In order to investigate the behavior of a reaction-diffusion system, a linear stability analysis around the fixed point (equilibrium) given by $\tilde{\mathbf{R}}(\tilde{\mathbf{x}}(t, r_1, r_2)) = 0$ is widely used. By linear approximation, (7) can be rewritten as follows

$$\begin{aligned} \frac{\partial \tilde{\mathbf{x}}_s(t, r_1, r_2)}{\partial t} &= \tilde{\mathbf{A}} \tilde{\mathbf{x}}_s(t, r_1, r_2) \\ &+ \tilde{\mathbf{D}} \nabla^2 \tilde{\mathbf{x}}_s(t, r_1, r_2), \end{aligned} \quad (8)$$

where

$\tilde{\mathbf{x}}_s(t, r_1, r_2)$: components of a small perturbation from the equilibrium,

$\tilde{\mathbf{A}}$: $N \times N$ matrix consisting of constants.

Taking the Laplace transform on 2-D space (r_1, r_2) , we have

$$\frac{\partial \tilde{\mathbf{X}}_s(t, s_1, s_2)}{\partial t} = \tilde{\mathbf{F}}(s_1, s_2) \tilde{\mathbf{X}}_s(t, s_1, s_2), \quad (9)$$

where

$$\tilde{\mathbf{F}}(s_1, s_2) = \tilde{\mathbf{A}} + (s_1^2 + s_2^2) \tilde{\mathbf{D}}.$$

In the above equation, $\tilde{\mathbf{X}}_s(t, s_1, s_2)$ denotes the Laplace transform of $\tilde{\mathbf{x}}_s(t, r_1, r_2)$, and s_1 and s_2 are complex frequencies. For simplicity, we assume that the matrix $\tilde{\mathbf{F}}$ has N distinct eigenvalues in the following discussion. Then, we can rewrite $\tilde{\mathbf{F}}$ in the form:

$$\tilde{\mathbf{F}}(s_1, s_2) = \tilde{\mathbf{P}}(s_1, s_2)\tilde{\mathbf{\Lambda}}(s_1, s_2)\tilde{\mathbf{P}}^{-1}(s_1, s_2), \quad (10)$$

where $\tilde{\mathbf{P}}$ is the matrix whose columns are the eigenvectors of $\tilde{\mathbf{F}}$, and $\tilde{\mathbf{\Lambda}}$ is the diagonal matrix of the eigenvalues given by

$$\tilde{\mathbf{\Lambda}}(s_1, s_2) = \begin{bmatrix} \tilde{\lambda}_1(s_1, s_2) & 0 & \cdots & 0 \\ 0 & \tilde{\lambda}_2(s_1, s_2) & 0 & \cdots & 0 \\ \vdots & \vdots & \ddots & & \vdots \\ 0 & 0 & \cdots & \tilde{\lambda}_N(s_1, s_2) \end{bmatrix}. \quad (11)$$

Using this representation, the solution of (9) can be written as

$$\begin{aligned} & \tilde{\mathbf{X}}_s(t, s_1, s_2) \\ &= \tilde{\mathbf{P}}(s_1, s_2) \exp[\tilde{\mathbf{\Lambda}}(s_1, s_2)t]\tilde{\mathbf{P}}^{-1}(s_1, s_2)\tilde{\mathbf{X}}_s(0, s_1, s_2). \end{aligned} \quad (12)$$

The solution (12) gives a non-stationary spatial pattern unless the dominant eigenvalue $\tilde{\lambda}_d(s_1, s_2)$ is real. Also, if the real part of $\tilde{\lambda}_d(s_1, s_2)$ is negative, then the spatial harmonics decays to zero. The condition that is capable of producing stationary spatial patterns is

$$\tilde{\lambda}_d(s_1, s_2) \in \mathfrak{R}, \quad \tilde{\lambda}_d(s_1, s_2) > 0, \quad (13)$$

for some $(s_1, s_2) = (j\omega_1, j\omega_2) \neq (0, 0)$, where \mathfrak{R} denotes the set of real numbers. Since the amplitude of every (ω_1, ω_2) satisfying the above condition grows as a function of time, the system becomes unstable. Therefore, in order to produce stationary spatial patterns, the system must be unstable for some $\omega_1, \omega_2 \neq 0$.

3. Digital Reaction-Diffusion System

This section defines a digital reaction-diffusion system (DRDS)—a model of a discrete-time discrete-space reaction-diffusion dynamical system having nonlinear reaction kinetics. The goal of this section is to show that the Turing’s pattern formation property can be naturally understood by the stability analysis of the DRDS within the framework of multidimensional digital signal processing theory.

3.1 Discretization of a Reaction-Diffusion System

We now sample a continuous variable $\tilde{\mathbf{x}}$ in (7) at the time sampling interval T_0 , and at the space sampling intervals T_1 and T_2 . Assuming discrete time-index to be given by n_0 and discrete space indices to be given by (n_1, n_2) , we have

$$\mathbf{x}(n_0, n_1, n_2) = \tilde{\mathbf{x}}(n_0T_0, n_1T_1, n_2T_2). \quad (14)$$

The general DRDS can be written as

$$\begin{aligned} & \mathbf{x}(n_0+1, n_1, n_2) \\ &= \mathbf{x}(n_0, n_1, n_2) + \mathbf{R}(\mathbf{x}(n_0, n_1, n_2)) \end{aligned}$$

$$+ \mathbf{D}(l * \mathbf{x})(n_0, n_1, n_2), \quad (15)$$

where

$$\begin{aligned} \mathbf{R} &= T_0 \tilde{\mathbf{R}} = [R_1(\mathbf{x}), R_2(\mathbf{x}), \dots, R_N(\mathbf{x})]^T, \\ \mathbf{D} &= T_0 \tilde{\mathbf{D}} = \text{diag}[D_1, D_2, \dots, D_N], \end{aligned}$$

$$l(n_1, n_2) = \begin{cases} \frac{1}{T_1^2} & (n_1, n_2) = (-1, 0), (1, 0) \\ \frac{1}{T_2^2} & (n_1, n_2) = (0, -1), (0, 1) \\ -2(\frac{1}{T_1^2} + \frac{1}{T_2^2}) & (n_1, n_2) = (0, 0) \\ 0 & \text{otherwise,} \end{cases}$$

and $*$ denotes the spatial convolution operator defined as

$$\begin{aligned} & (l * \mathbf{x})(n_0, n_1, n_2) \\ &= \begin{bmatrix} (l * x_1)(n_0, n_1, n_2) \\ (l * x_2)(n_0, n_1, n_2) \\ \vdots \\ (l * x_N)(n_0, n_1, n_2) \end{bmatrix} \\ &= \begin{bmatrix} \sum_{p_1=-1}^1 \sum_{p_2=-1}^1 l(p_1, p_2)x_1(n_0, n_1 - p_1, n_2 - p_2) \\ \sum_{p_1=-1}^1 \sum_{p_2=-1}^1 l(p_1, p_2)x_2(n_0, n_1 - p_1, n_2 - p_2) \\ \vdots \\ \sum_{p_1=-1}^1 \sum_{p_2=-1}^1 l(p_1, p_2)x_N(n_0, n_1 - p_1, n_2 - p_2) \end{bmatrix}. \end{aligned}$$

This gives the basic form of DRDS.

3.2 Linear Stability Analysis of DRDS

In this subsection, we derive the condition for DRDS to have a pattern formation capability which is equivalent to the Turing’s diffusion-instability condition. By linearizing the system around the equilibrium ($\mathbf{R}(\mathbf{x}) = 0$), (15) can be written as

$$\begin{aligned} & \mathbf{x}_s(n_0+1, n_1, n_2) \\ &= \mathbf{x}_s(n_0, n_1, n_2) + \mathbf{A}\mathbf{x}_s(n_0, n_1, n_2) \\ &+ \mathbf{D}(l * \mathbf{x}_s)(n_0, n_1, n_2), \end{aligned} \quad (16)$$

where

$\mathbf{x}_s(n_0, n_1, n_2)$: components of a small perturbation from the equilibrium,

\mathbf{A} : $N \times N$ matrix consisting of constants.

By taking z -transform over 2-D space (n_1, n_2) , we have

$$\mathbf{X}_s(n_0 + 1, z_1, z_2)$$

$$= (\mathbf{I} + \mathbf{F}(z_1, z_2))\mathbf{X}_s(n_0, z_1, z_2), \quad (17)$$

where

$$\mathbf{F}(z_1, z_2) = \mathbf{A} + \left\{ \frac{(z_1 - 2 + z_1^{-1})}{T_1^2} + \frac{(z_2 - 2 + z_2^{-1})}{T_2^2} \right\} \mathbf{D}.$$

Applying (17) recursively, we have

$$\mathbf{X}_s(n_0, z_1, z_2) = (\mathbf{I} + \mathbf{F}(z_1, z_2))^{n_0} \mathbf{X}_s(0, z_1, z_2). \quad (18)$$

Assuming that the above equation represents a digital system whose input is $\mathbf{X}_s(0, z_1, z_2)$ and output is $\mathbf{X}_s(n_0, z_1, z_2)$, the term $(\mathbf{I} + \mathbf{F}(z_1, z_2))^{n_0}$ can be viewed as the n_0 -step transfer function from the input to the output.

In the following, we will derive the simplified expression of the n_0 -step transfer function. For simplicity, we suppose here that the matrix \mathbf{F} has N distinct eigenvalues. In this case, we can rewrite \mathbf{F} as

$$\mathbf{F}(z_1, z_2) = \mathbf{P}(z_1, z_2)\mathbf{\Lambda}(z_1, z_2)\mathbf{P}^{-1}(z_1, z_2), \quad (19)$$

where \mathbf{P} is the matrix whose columns are the eigenvectors of \mathbf{F} , and $\mathbf{\Lambda}$ is the diagonal matrix consisting of eigenvalues of \mathbf{F} given by

$$\mathbf{\Lambda}(z_1, z_2) = \begin{bmatrix} \lambda_1(z_1, z_2) & 0 & \cdots & 0 \\ 0 & \lambda_2(z_1, z_2) & 0 & \cdots & 0 \\ \vdots & \vdots & \ddots & & \vdots \\ 0 & 0 & \cdots & \lambda_N(z_1, z_2) \end{bmatrix}. \quad (20)$$

Then, the n_0 -step transfer function can be represented as

$$\begin{aligned} & (\mathbf{I} + \mathbf{F}(z_1, z_2))^{n_0} \\ &= \mathbf{P}(z_1, z_2)(\mathbf{I} + \mathbf{\Lambda}(z_1, z_2))^{n_0}\mathbf{P}^{-1}(z_1, z_2), \end{aligned} \quad (21)$$

where

$$\begin{aligned} & (\mathbf{I} + \mathbf{\Lambda}(z_1, z_2))^{n_0} \\ &= \begin{bmatrix} (1 + \lambda_1(z_1, z_2))^{n_0} & 0 & \cdots & 0 \\ 0 & (1 + \lambda_2(z_1, z_2))^{n_0} & 0 & \cdots & 0 \\ \vdots & \vdots & \ddots & & \vdots \\ 0 & 0 & \cdots & (1 + \lambda_N(z_1, z_2))^{n_0} \end{bmatrix}. \end{aligned}$$

We can prove that the Turing's instability condition is equivalent to the condition that the n_0 -step transfer function becomes non-oscillatory (real) and unstable. That is, the dominant eigenvalue $\lambda_d(z_1, z_2)$ in (20) must be real and positive:

$$\lambda_d(z_1, z_2) \in \Re, \quad \lambda_d(z_1, z_2) > 0, \quad (22)$$

for some $w_1, w_2 \neq 0$, where $z_1 = e^{j\omega_1 T_1}$ and $z_2 = e^{j\omega_2 T_2}$. Since the amplitude of a wave having the spatial frequencies ω_1 and ω_2 satisfying the above condition grows

Table 1 Classification of patterns generated by DRDS according to eigenvalue λ_i .

λ_i	Every $Re[\lambda_i] < 0$ (stable)	Some $Re[\lambda_i] > 0$ (unstable)
Complex	Decaying Oscillatory	Growing Oscillatory
Real	Decaying Non-oscillatory	Growing Non-oscillatory

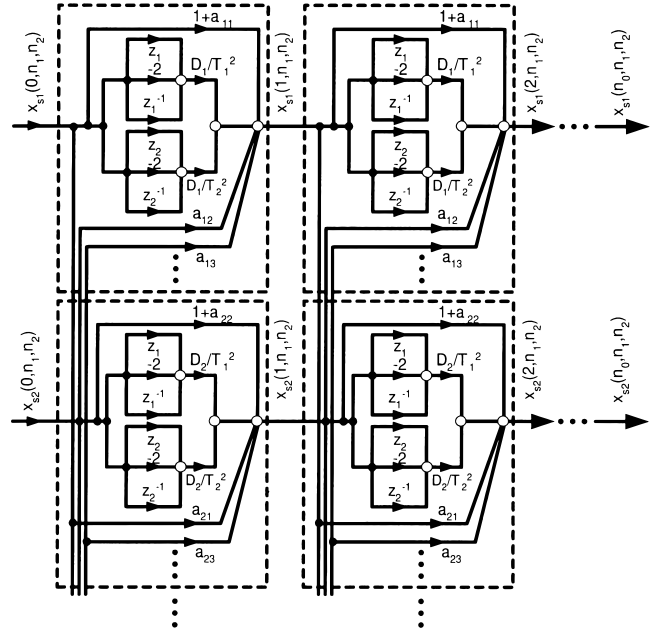


Fig. 1 Flow diagram for an N morphogen DRDS.

as a function of time, DRDS develops 2-D concentration patterns $\mathbf{x}_s(n_0, n_1, n_2)$ having the specified spatial frequencies. Table 1 shows the classification of patterns generated by DRDS according to the eigenvalue λ_i . The growing non-oscillatory case could develop stationary Turing patterns when adequate non-linear functions are employed.

From the view point of digital signal processing, the linearized form of DRDS (17) can be understood as a 2-D linear digital filter, where $\mathbf{X}_s(n_0, z_1, z_2)$ is the input (z -transformed form), $\mathbf{X}_s(n_0 + 1, z_1, z_2)$ is the output (z -transformed form), and $(\mathbf{I} + \mathbf{F}(z_1, z_2))$ is the 2-D transfer function. The output of this 2-D digital filter is recursively fed back to its input as the time index n_0 increases. The instability condition (22) can be understood as the condition that the 2-D transfer function $(\mathbf{I} + \mathbf{F}(z_1, z_2))$ becomes unstable. Thus, the linear analysis of DRDS is closely related to the theoretical study of multidimensional digital filters.

Assume that $\mathbf{x}_s(n_0, n_1, n_2) = [x_{s1}(n_0, n_1, n_2), \dots, x_{sN}(n_0, n_1, n_2)]^T$, and that a_{ij} denotes the (i, j) -element of the $N \times N$ matrix \mathbf{A} . Figure 1 shows the equivalent digital filter structure for the "linearized" DRDS, where the structure is unfolded for the discrete time index n_0 . In practical situation, we first store

an initial (input) image in a specific morphogen, say $x_{si}(0, n_1, n_2)$, at time 0. After computing the dynamics for n_0 steps, we can obtain the output image from one of the N morphogens at time n_0 . Assume that we obtain the output image from $x_{si}(n_0, n_1, n_2)$ for typical situation. As illustrated in Fig. 1, the n_0 -step transfer function from the input $x_{si}(0, n_1, n_2)$ to the output $x_{si}(n_0, n_1, n_2)$ becomes a composite function of the N basic filter functions indicated by the dashed-line boxes in Fig. 1. As the number of morphogens N increases, the variety of basic filters increases, resulting in significant increase in the complexity of the total transfer function.

This n_0 -step transfer function is represented by the matrix form (21). If we increase the number of morphogens, the number of modes $(1 + \lambda_i(z_1, z_2))^{n_0}$ ($i = 1, \dots, N$) appeared in (21) increases. For a linear system, its asymptotic behavior is determined by the dominant mode $(1 + \lambda_d(z_1, z_2))^{n_0}$ having the largest eigenvalue λ_d . In general, however, we assume the use of non-linear reaction kinetics for DRDS whose phase-space trajectory is bounded within a finite domain, which suppresses infinite growth of the dominant mode. Hence, if we increase the number of morphogens, it is likely that the N different modes exhibit cooperative behavior to develop highly complex spatial patterns.

For practical applications, there are various different ways of selecting input/output morphogens. Note that each of N morphogens $x_{s1}(n_0, n_1, n_2), \dots, x_{sN}(n_0, n_1, n_2)$ can be represented by a linear combination of N distinct modes as suggested by (21), hence there is no essential difference among their pattern formation capabilities in small-signal (linear) context. However, the real problem can become more complicated, since non-linear reaction functions are used in DRDS. Thus, we must carry out intensive simulation study to determine the optimal input/output pair of morphogens as well as other design parameters in practical applications.

3.3 DRDS with Brusselator Reaction Kinetics

We illustrate Turing's mechanism of pattern formation in the DRDS employing the "Brusselator" reaction function, which is one of the most widely studied chemical oscillator [1]. Consider the two-species DRDS given by (15) with $N = 2$. We shall define the Brusselator-based reaction kinetics for DRDS as

$$\begin{aligned} \mathbf{R}(\mathbf{x}) &= T_0 \tilde{\mathbf{R}}(\tilde{\mathbf{x}}) \\ &= T_0 \begin{bmatrix} k_1 - (k_2 + 1)x_1 + x_1^2 x_2 \\ k_2 x_1 - x_1^2 x_2 \end{bmatrix}. \end{aligned} \quad (23)$$

We can predict the behavior of DRDS (15) employing the linear stability analysis technique described in the previous subsection. We can prove that the condition (22) can be written as

$$\begin{aligned} &16D_1 D_2 \left(\frac{1}{T_1^2} \sin^2 \frac{\omega_1 T_1}{2} + \frac{1}{T_2^2} \sin^2 \frac{\omega_2 T_2}{2} \right)^2 \\ &\quad - 4\{-T_0 k_1^2 D_1 + T_0(k_2 - 1)D_2\} \\ &\quad \times \left(\frac{1}{T_1^2} \sin^2 \frac{\omega_1 T_1}{2} + \frac{1}{T_2^2} \sin^2 \frac{\omega_2 T_2}{2} \right) \\ &\quad + T_0^2 k_1^2 < 0. \end{aligned} \quad (24)$$

That is, if the above condition is satisfied, the dynamics develops spatial patterns. For example, consider the parameter set: $k_1 = 2, k_2 = 4, T_0 = 0.01, D_1 = 0.01, D_2 = 0.05$, and $T_1 = T_2 = 1$. In this case, the total dynamics can be represented as

$$\begin{cases} x_1(n_0 + 1, n_1, n_2) \\ \quad = 0.02 + 0.01x_1^2(n_0, n_1, n_2)x_2(n_0, n_1, n_2) \\ \quad \quad + 0.95x_1(n_0, n_1, n_2) \\ \quad \quad + 0.01(l * x_1)(n_0, n_1, n_2) \\ x_2(n_0 + 1, n_1, n_2) \\ \quad = -0.01x_1^2(n_0, n_1, n_2)x_2(n_0, n_1, n_2) \\ \quad \quad + 0.04x_1(n_0, n_1, n_2) + x_2(n_0, n_1, n_2) \\ \quad \quad + 0.05(l * x_2)(n_0, n_1, n_2) \end{cases} \quad (25)$$

This dynamics satisfies the pattern formation condition (24) for the frequency band $0.115 \leq \sin^2 \frac{\omega_1}{2} + \sin^2 \frac{\omega_2}{2} \leq 0.435$. Figure 2 is the computer simulation showing the system develops the 2-D structures of characteristic spatial frequencies, which is triggered off by random disturbances.

3.4 Enhancement of Fingerprint Images with DRDS

This subsection presents the application of DRDS to processing of fingerprint images. Figure 3 shows the construction of the system, where Brusselator-based DRDS defined by (25) is employed. In this case, the dynamics has the equilibrium $(x_1, x_2) = (2, 2)$, and the variation ranges of variables (x_1, x_2) are bounded around the equilibrium point as $1 \leq x_1 \leq 3$ and $1 \leq x_2 \leq 3$. Hence, we first scale the $[0, 255]$ gray-scale image into $[1, 3]$ range. The scaled image becomes the initial input for the 1st morphogen $x_1(0, n_1, n_2)$, while the initial condition of the 2nd morphogen is given by $x_2(0, n_1, n_2) = 2$ (equilibrium). The zero-flux Neumann boundary condition is employed for computing the dynamics. After n_0 steps of DRDS computation, we obtain $x_1(n_0, n_1, n_2)$ as the output image, which is scaled back into the $[0, 255]$ gray-scale image to produce the final output.

Example 1: *Enhancement of a fingerprint image*

We demonstrate here an example of fingerprint enhancement using Brusselator-based DRDS. We use dynamics (25), but adjusted the spatial sampling parameters as $T_1 = 0.6863$ and $T_2 = 0.5759$ corresponding to the inherent spatial frequency of the given fingerprint image. Note that a typical fingerprint image has

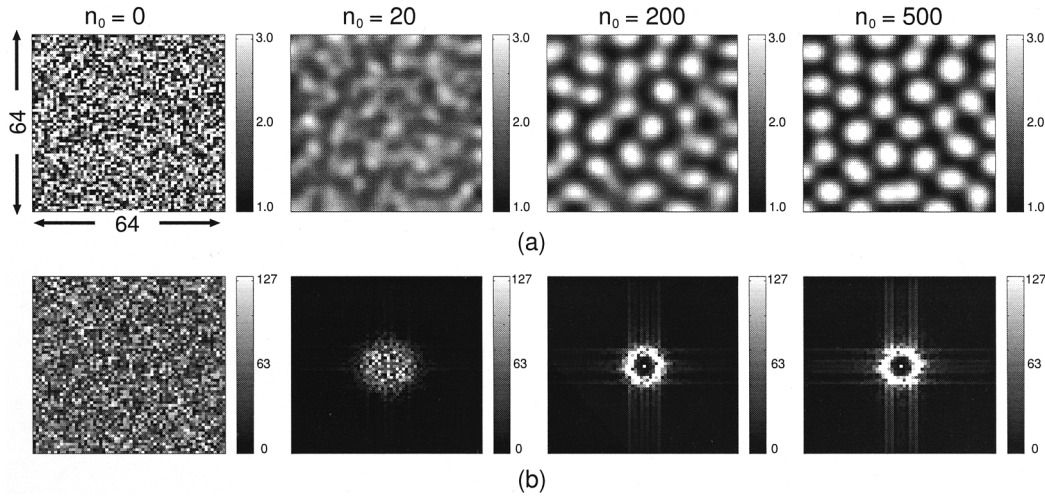


Fig. 2 Formation of a Turing pattern using DRDS with Brusselator reaction kinetics: (a) time evolution of the concentration $x_1(n_0, n_1, n_2)$, (b) the corresponding amplitude spectra in frequency domain.

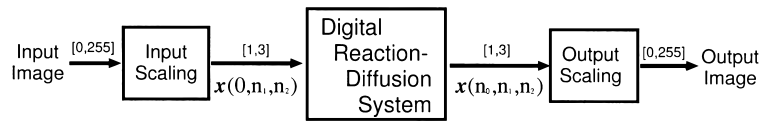


Fig. 3 System block diagram.

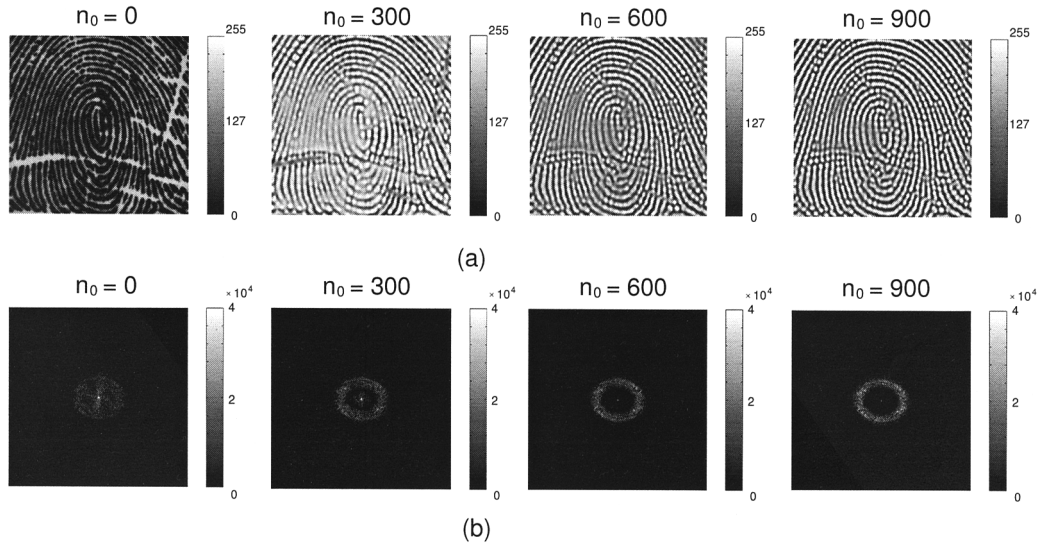


Fig. 4 Enhancement of a fingerprint image: (a) time evolution of concentration $x_1(n_0, n_1, n_2)$, (b) the corresponding amplitude spectra in frequency domain.

an elliptic spectral distribution in frequency domain (ω_1, ω_2) . Every fingerprint has its own combination of horizontal/vertical spatial frequency components. For effective enhancement of a given fingerprint image, we must adjust the unstable frequency band of DRDS to cover the dominant frequency components of the given fingerprint image. The parameters T_1 and T_2 are particularly useful for this purpose. Smaller T_1 and T_2

imply a larger radius of unstable frequency band. Figure 4(a) shows the input fingerprint image $x_1(0, n_1, n_2)$ (256×256 pixels) and the output images $x_1(n_0, n_1, n_2)$ at time steps $n_0 = 300, 600$ and 900 , respectively. Figure 4(b) shows the corresponding amplitude spectra. The inherent spatial frequency components of the given fingerprint image is enhanced significantly by the pattern formation capability of DRDS. \square

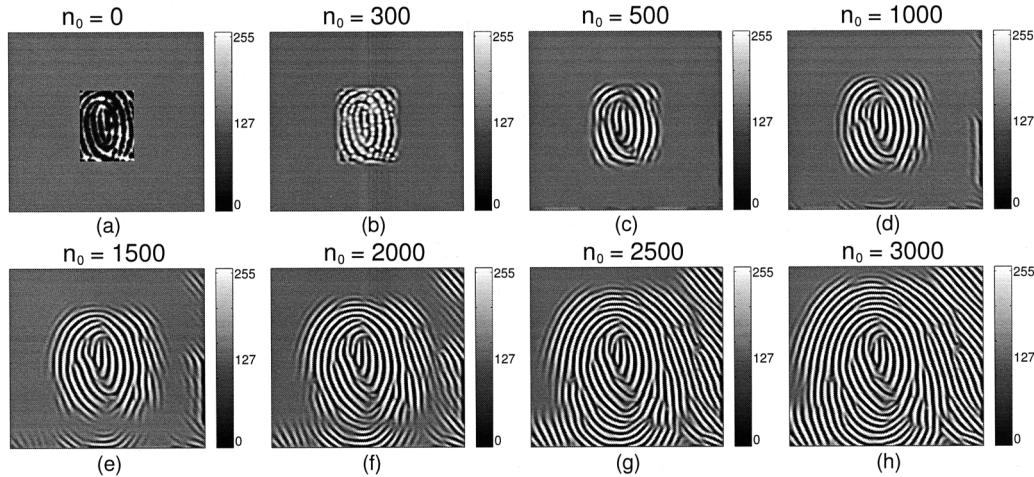


Fig. 7 Restoration of a fingerprint image: (a) input image, (b)–(h) restored image by using adaptive DRDS.

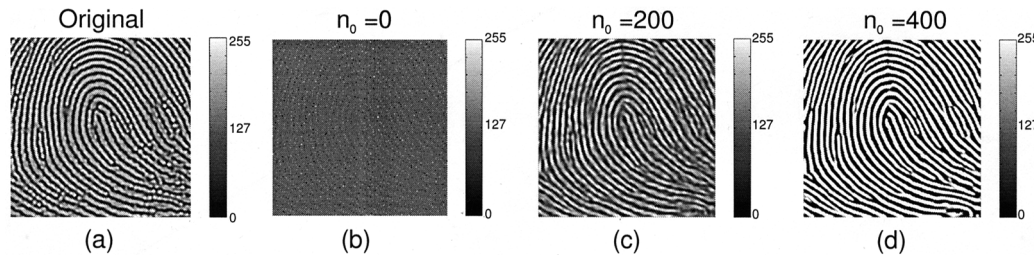


Fig. 8 Reconstruction of a fingerprint pattern from a subsampled image: (a) original image, (b) 1/16 subsampled image, (c) and (d) restored image using adaptive DRDS.

adaptive DRDS processing, we have the final output $x_1(600, n_1, n_2)$ as shown in (d). Thus, the use of orientation masks in the adaptive DRDS makes possible significant improvement in image quality, in comparison with that of the original DRDS (Fig. 4(a)). \square

Example 3: Restoration of a fingerprint image

Assume that only the center part of the fingerprint image used in Example 2 is given as shown in Fig. 7(a), and that all the orientation masks extracted in Example 2 are available. Even under such condition, the adaptive DRDS can restore the whole fingerprint pattern as shown in Figs. 7(b)–(h), where the fingerprint spreads out from the center under the guidance of the orientation masks. \square

This example assumes the use of orientation masks extracted in advance. In many applications, however, it is likely that the information of local orientation must be extracted from the blurred input image. The following example considers such situation, where a low-quality fingerprint image is given and the system must reconstruct the complete fingerprint pattern without any additional information.

Example 4: Reconstruction of fingerprint patterns from subsampled images

We consider here the problem of restoring the original fingerprint image from the subsampled image. The

adaptive DRDS used here employs the same reaction kinetics and parameters as in Examples 2 and 3. The input image is obtained by subsampling the original fingerprint image by the subsampling rate 1/16. This process reduces the number of pixels by 1/16. Figures 8(a) and (b) show the original image and the subsampled image, respectively. The system first extracts the local orientation information from the subsampled image (b), and generates orientation masks to guide the action of adaptive DRDS. Figure 8(d) shows the output $x_1(400, n_1, n_2)$ of the adaptive DRDS.

Figure 9 shows the correlation score (similarity) between the original fingerprint image and the output of adaptive DRDS for four different fingerprint samples. To calculate similarity between the two fingerprint images (the original image and the restored image), we use *phase-only correlation* technique [6]. The phase-only correlation function has an efficient discrimination capability for fingerprint images, as demonstrated in recent commercial products of fingerprint-matching devices [6]. The correlation score plotted in Fig. 9 is calculated by taking the sum of the ten highest values of the 2-D phase-only correlation function of two images. For every fingerprint sample, we can confirm that the similarity between the original image and the restored image $x_1(n_0, n_1, n_2)$ increases as the number of

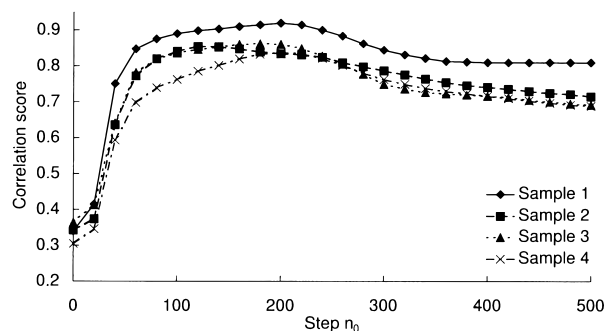


Fig. 9 Correlation between the original image and the restored image.

steps n_0 increases. The highest correlation score > 0.8 is observed around $n_0 = 200$ steps for every fingerprint sample. After the peak, the correlation score gradually decreases as the time index n_0 increases. This is because the input image is stored only in the initial state variable $x_1(0, n_1, n_2)$, and the recursive dynamics gradually deforms the original shape of the fingerprint as the number of processing steps increases. Recently, we have investigated the possibility of improving the recognition capability for blurred fingerprint images by using the DRDS-based restoration technique. An interesting observation is that the optimal discrimination capability could be obtained around $n_0 = 400$ – 500 rather than at the step of the highest correlation score. In the range of $n_0 = 400$ – 500 , the correlation scores for the wrong fingerprints drop steeply while the correct fingerprint keeps sufficient level of correlation. Although further analysis is required for practical application, this example demonstrates a potential capability of adaptive DRDS to enhance the performance of matching algorithms for blurred fingerprint images. \square

5. Conclusion

This paper presents a digital reaction-diffusion system (DRDS)—a model of a discrete-time discrete-space reaction-diffusion dynamical system—useful for signal processing and computer graphics applications. This paper also describes the design of an adaptive DRDS having the capability to reconstruct a complete fingerprint pattern from a blurred image. We are expecting that the framework of DRDS may provide a theoretical foundation of *digital morphogenesis*, that is, a technique for applying the principle of biological pattern formation phenomena to many engineering problems.

References

- [1] J.D. Murray, *Mathematical biology*, Springer-Verlag, Berlin, 1993.
- [2] S. Kondo and R. Asai, “A reaction-diffusion wave on the skin of the marine angelfish pomacanthus,” *Nature*, vol.376, pp.765–768, Aug. 1995.
- [3] K.R. Crouse and L.O. Chua, “Methods for image processing and pattern formation in cellular neural networks: A tutorial,” *IEEE Trans. Circuits & Syst.-I*, vol.42, no.10, pp.583–601, Oct. 1995.
- [4] L. Goras, L.O. Chua, and L. Pivka, “Turing patterns in CNNs—Part II: Equations and behaviors,” *IEEE Trans. Circuits & Syst.-I*, vol.42, no.10, pp.612–626, Oct. 1995.
- [5] A.S. Sherstinsky and R.W. Picard, “M-lattice: From morphogenesis to image processing,” *IEEE Trans. Image Processing*, vol.5, no.7, pp.1137–1150, July 1996.
- [6] K. Kobayashi, H. Nakajima, T. Aoki, M. Kawamata, and T. Higuchi, “Principles of phase only correlation and its applications,” *ITE Technical Report*, vol.20, no.41, pp.1–6, July 1996.



Koichi Ito received the B.E. degree in electronic engineering from Tohoku University, Sendai, Japan, in 2000. He is currently working toward the M.E. degree. His research interest includes nonlinear digital signal processing and computer graphics. Mr. Ito received the Tohoku Section Presentation Award from Information Processing Society of Japan in 2000.



Takafumi Aoki received the B.E., M.E., and D.E. degrees in electronic engineering from Tohoku University, Sendai, Japan, in 1988, 1990, and 1992, respectively. He is currently an Associate Professor of the Graduate School of Information Sciences at Tohoku University. For 1997–1999, he also joined the PRESTO project, Japan Science and Technology Corporation (JST). His research interests include theoretical aspects of computa-

tion, VLSI computing structures for signal and image processing, multiple-valued logic, and biomolecular computing. Dr. Aoki received the Outstanding Paper Award at the 1990, 2000, and 2001 IEEE International Symposiums on Multiple-Valued Logic, the Outstanding Transactions Paper Award from the Institute of Electronics, Information and Communication Engineers (IEICE) of Japan in 1989 and 1997, the IEE Ambrose Fleming Premium Award in 1994, the IEICE Inose Award in 1997, the IEE Mountbatten Premium Award in 1999, and the Best Paper Award at the 1999 IEEE International Symposium on Intelligent Signal Processing and Communication Systems.



Tatsuo Higuchi received the B.E., M.E., and D.E. degrees in electronic engineering from Tohoku University, Sendai, Japan, in 1962, 1964, and 1969, respectively. He is currently a Professor, and was Dean from 1994 to 1998 in the Graduate School of Information Sciences at Tohoku University. From 1980 to 1993, he was a Professor in the Department of Electronic Engineering at Tohoku University. His general research interests in-

clude the design of 1-D and multi-D digital filters, linear time-varying system theory, fractals and chaos in digital signal processing, VLSI computing structures for signal and image processing, multiple-valued ICs, multiwave opto-electronic ICs, and biomolecular computing. Dr. Higuchi received the Outstanding Paper Awards at the 1985, 1986, 1988, 1990, 2000, and 2001 IEEE International Symposiums on Multiple-Valued Logic, the Outstanding Transactions Paper Award from the Society of Instrument and Control Engineers (SICE) of Japan in 1984, the Technically Excellent Award from SICE in 1986, and the Outstanding Book Award from SICE in 1996, the Outstanding Transactions Paper Award from the Institute of Electronics, Information and Communication Engineers (IEICE) of Japan in 1990 and 1997, the Inose Award from IEICE in 1997, the Technically Excellent Award from the Robotics Society of Japan in 1990, the IEE Ambrose Fleming Premium Award in 1994, the Outstanding Book Award from the Japanese Society for Engineering Education in 1997, the Award for Persons of scientific and technological merits (Commendation by the minister of state for Science and Technology), the IEE Mountbatten Premium Award in 1999 and the Best Paper Award at the 1999 IEEE International Symposium on Intelligent Signal Processing and Communication Systems. He also received the IEEE Third Millennium Medal in 2000. He received the fellow grade from IEEE, IEICE, and SICE.